ARL-MR-1056 ● SEP 2022

Photoresist Optimization for Lead Zirconate Titanate (PZT) Processing and Devices

by Daniel M Potrepka

Approved for public release: distribution unlimited.

NOTICES

Disclaimers

The findings in this report are not to be construed as an official Department of the Army position unless so designated by other authorized documents.

Citation of manufacturer's or trade names does not constitute an official endorsement or approval of the use thereof.

Destroy this report when it is no longer needed. Do not return it to the originator.

ARL-MR-1056 ● SEP 2022

Photoresist Optimization for Lead Zirconate Titanate (PZT) Processing and Devices

Daniel M Potrepka
DEVCOM Army Research Laboratory

Approved for public release: distribution unlimited.

REPORT DOCUMENTATION PAGE			*Form Approved* *OMB No. 0704-0188*

Public reporting burden for this collection of information is estimated to average 1 hour per response, including the time for reviewing instructions, searching existing data sources, gathering and maintaining the data needed, and completing and reviewing the collection information. Send comments regarding this burden estimate or any other aspect of this collection of information, including suggestions for reducing the burden, to Department of Defense, Washington Headquarters Services, Directorate for Information Operations and Reports (0704-0188), 1215 Jefferson Davis Highway, Suite 1204, Arlington, VA 22202-4302. Respondents should be aware that notwithstanding any other provision of law, no person shall be subject to any penalty for failing to comply with a collection of information if it does not display a currently valid OMB control number.

PLEASE DO NOT RETURN YOUR FORM TO THE ABOVE ADDRESS.

1. REPORT DATE *(DD-MM-YYYY)*	**2. REPORT TYPE**	**3. DATES COVERED (From - To)**
September 2022	Memorandum Report	1 December 2021–31 May 2022

4. TITLE AND SUBTITLE	**5a. CONTRACT NUMBER**
Photoresist Optimization for Lead Zirconate Titanate (PZT) Processing and Devices	
	5b. GRANT NUMBER
	5c. PROGRAM ELEMENT NUMBER
6. AUTHOR(S)	**5d. PROJECT NUMBER**
Daniel M Potrepka	
	5e. TASK NUMBER
	5f. WORK UNIT NUMBER
7. PERFORMING ORGANIZATION NAME(S) AND ADDRESS(ES)	**8. PERFORMING ORGANIZATION REPORT NUMBER**
DEVCOM Army Research Laboratory ATTN: FCDD-RLS-SA Adelphi, MD 20783	ARL-MR-1056
9. SPONSORING/MONITORING AGENCY NAME(S) AND ADDRESS(ES)	**10. SPONSOR/MONITOR'S ACRONYM(S)**
	11. SPONSOR/MONITOR'S REPORT NUMBER(S)

12. DISTRIBUTION/AVAILABILITY STATEMENT

Approved for public release: distribution unlimited.

13. SUPPLEMENTARY NOTES

ORCID ID: Daniel M Potrepka, 0000-0002-0528-1038

14. ABSTRACT

This study focused on resolving defects in photoresist patterns after UV curing that affect device feature quality and electromechanical performance. Designs of experiments (DOEs) were performed to obtain photoresist profiles for the AZ 5214 positive photoresist process with a 2,000-rpm spin during dispense. These profiles were then analyzed by a confocal microscope, a stylus profilometer, and scanning electron microscopy. The specific problems with the patterns revealed by the DOE and analysis are discussed. A plan forward is then discussed listing options that could lead to further photoresist and device–feature optimization for enhanced performance.

15. SUBJECT TERMS

Mechanical Sciences; Photonics, Electronics, and Quantum Sciences; photoresist; UV cure; microelectronics; piezoelectric MEMS; process characterization

16. SECURITY CLASSIFICATION OF:			**17. LIMITATION OF ABSTRACT**	**18. NUMBER OF PAGES**	**19a. NAME OF RESPONSIBLE PERSON**
					Daniel M Potrepka
a. REPORT	**b. ABSTRACT**	**c. THIS PAGE**			**19b. TELEPHONE NUMBER (Include area code)**
Unclassified	Unclassified	Unclassified	UU	28	(301) 394-0389

Standard Form 298 (Rev. 8/98)
Prescribed by ANSI Std. Z39.18

Contents

List of Figures iv

List of Tables v

Acknowledgments

1. Introduction 1

2. Experiment 2

3 Results/Discussion 4

3.1 Stylus Profilometry of Wide and Narrow Linewidths 4

3.2 SEM Images 10

3.3 Options for Optimization Paths Forward 11

3.3.1 UV Cure Optimization of the Axcelis Process 11

3.3.2 Hard Bake Alternatives 12

3.3.3 G-, H-, and I-Line Sensitive Photoresists 15

4. Summary and Conclusion 16

5. References 17

List of Symbols, Abbreviations, and Acronyms 18

Distribution List 20

List of Figures

Fig. 1 Profilometer scan of the 60-µm (nominal) photoresist line for Wafer 1 (no UV cure) 5

Fig. 2 Slope of the profilometer scan in Fig. 1. Gaps in the plot are an artifact in the local calculation of the derivative. 5

Fig. 3 Profilometer scan of the 60-µm (nominal) photoresist line for Wafer 2 (with UV cure). Measurement lengths corner-to-corner for Table 2 are illustrated as the red and green lines. 6

Fig. 4 Slope of the profilometer scan in Fig. 3. Gaps in the plot are an artifact in the local calculation of the derivative. 6

Fig. 5 Profilometer scan of the 10-µm (nominal) photoresist line for Wafer 1 (no UV cure) 7

Fig. 6 Slope of the profilometer scan in Fig. 5. Gaps in the plot are an artifact in the local calculation of the derivative. 7

Fig. 7 Profilometer scan of the 10-µm (nominal) photoresist line for Wafer 2 (with UV cure) 8

Fig. 8 Slope of the profilometer scan in Fig. 7 8

Fig. 9 Relationship between the line schematic cross-sectional view and the line profile 10

Fig. 10 Uncured photoresist (Wafer 1) 10

Fig. 11 UV cured photoresist (Wafer 2) 11

Fig. 12 A hard bake typically triggers various physical and chemical reactions in a resist film. At temperatures above 140 °C, positive resist film structures cross-link to increase their chemical stability for subsequent process steps 13

Fig. 13 The thermal softening (reflow) of developed rectangular resist structures from AZ 40XT at different temperatures and times for 80-µm resist film thickness (above) and 50-µm resist film thickness (below). 13

Fig. 14 Cross sections of thermally softened AZ ECI 3027 resist structures for increasing temperature, left to right 14

Fig. 15 Spectral sensitivity of AZ photoresists 15

List of Tables

Table 1 Axcelis process for program Ron-200C 3

Table 2 Critical dimensions for the KLA Tencor P-15 profilometer scans obtained with a 2-µm stylus... 9

Table 3 Ramp rates and temperature plateaus used 12

Table 4 Frequency ranges of relative photoactivation 15

Acknowledgments

Daniel M Potrepka gratefully acknowledges the following DEVCOM ARL personnel: Mr Joel L Martin for the several discussions on the Axcelis and team photoprocesses; Ms Ana N Cohen for many discussions, retraining support, and technical services assistance with photoprocessing technology; Ms Glynis S Sullivan for several technical and equipment discussions; Dr Robert R Benoit for assistance to coordinate team and project goals; and Dr Paul D Sunal for numerous suggestions to enhance the relevance of the technical content, experimental design, and cleanroom technical service support and collaborations.

1. Introduction

Why do we use UV cure? Among other applications, UV cure of photoresist improves resistance to physical milling, plasma, and chemicals for photoresist used as a blocking mask to protect device features that are being defined during dry etching.[1] UV cure can also enhance charge neutralization on the photoresist surface and relieve stress.[1] Simply put, the UV cure adds to the ability to strengthen the photoresist so that it better protects regions covered by it against process damage in the processing of device features. The Piezoelectric Microelectromechanical Systems (PiezoMEMS) team at the US Army Combat Capabilities Development Command Army Research Laboratory has a particular interest in UV-cured photoresist for its lead zirconate titanate (PZT) and other piezoelectric-driven MEMS device applications.

Geometric features of devices produced by the PiezoMEMS team have experienced problems that affect performance of the fabricated devices, particularly in weakened regions of the resist along the edges and into the body of the resist pattern. This can lead to unintended etching into the device region.

Specifically, etching in ion mill or deep silicon etch (DSE) incompletely reproduces mask features in the device using UV-cured photoresist for masking against the milling issues that impact electrical function and thus deteriorate device performance. Despite such breakdown, the UV cure is essential to provide the protective function of the resist. The goal of this research is to optimize the UV-cured resist to create a uniform and robust photoresist mask.

Azoplate AZ 5214 photoresist was deposited on two 150-mm-diameter single-crystal silicon (Si) test wafers with native silicon dioxide (SiO_2) surfaces. The resist was then patterned. One received UV cure, the other did not. Confocal microscope imaging qualitatively verified pattern quality in a preliminary microscopic inspection. Profilometry revealed changes in the sidewall cross section after UV cure compared to the uncured AZ 5214. Scanning electron microscopy (SEM) images showed that the sidewall profile exhibited nonuniformities after UV cure, whereas uncured AZ 5214 had smooth uniform sidewalls. Quantitative profile features such as slope, linewidth, nominal nonuniformity feature size, and landscape of nonuniformity features in the profilometer and SEM scans are discussed. Methods for optimization of the photoresist profile are based on these results, procedures discussed in the literature, and subject-matter experts in the lab. All of this feedback is used to inform the next design of experiments (DOE) for further refinement.

2. Experiment

A DOE was created to process a control sample of photoresist without a UV cure and a process sample of photoresist with a UV cure. The two starting substrates were Si 400 wafers with a native oxide surface. A backside scribe identified them with the number 1 and 2, for no resist curing and UV cure, respectively. AZ 5214 was first deposited on a dummy (pilot) wafer, and then having seen good-quality photoresist on the pilot wafer, onto Wafers 1 and 2 using the EVG 120 Resist Processing Cluster program 6C5214_2K (6 for 6-inch wafer, C for coating, 5214 for the AZ resist type, and 2K for 2,000-rpm resist spin speed after dispensing the resist onto the wafer). In the process, the wafer is first exposed to a vapor of hexamethyldisilazane (HMDS) surfactant. Then, the wafer is soft baked at about 95 °C for about 1–2 min. The AZ 5214 resist is then flooded onto the wafer and then spun at 2,000 rpm for about 30 s, then hard baked at about 110 °C for about 1–2 min.

Photoexpose was performed using the 02_AlN in the pQMGv3 mask of the QMGv3 device's mask set. Using the Karl Suss MA6 / BA6 Contact Aligner in Vacuum Contact mode, the photoresist on Wafers 1 and 2 was exposed at constant intensity for 6.7 s to receive a dose of about 60 mJ/cm^2. The wafers were then developed using the program 6D300_60 (6 inch, develop, AZ 300, 60 s). An edge bead removal was performed using the program 6EBR_2mm. The develop program essentially sprays the wafer at spin speed to flood it with the developer, then rinses with deionized water and ramps the spin speed up to dry it off.

The wafers were then visually inspected for quality and further checked using an optical light microscope and an Olympus LEXT laser confocal microscope.

Using the cure program Ron-200C (which is tailored for processing the 2-µm thick photoresist) in the Axcelis UV Photoresist Stabilizer process tool, a dummy (pilot) wafer was first processed. Then Wafer 2 was processed. The program loads the wafer into the chamber. The photoresist is hardened (cured) by exposing it to UV radiation while subjecting it to elevated temperatures similar to the process discussed in Takacs et al.[2] During this process, it ramps the temperature to 110 °C and holds, then to 150 °C, then to 170 °C, then to 200 °C, then cooling, and then the wafer is removed from the chamber. The process details are displayed in Table 1.

Table 1 Axcelis process for program Ron-200C

T (°C)	t (s)
110	50
R_{UP}	20
150	10
R_{UP}	20
170	10
R_{UP}	20
200	10
R_{DWN}	…

Optical microscope inspection was again performed on Wafer 2 after the Axcelis UV cure. A confocal microscope measurement was made on the surfaces of Wafers 1 and 2 to observe overall photoresist quality for several dies in the middle of the wafer and along a circle with about a 1.5-inch radius from the wafer center.

Stylus profilometer scans were made over a selected large and small critical dimension: about 60-µm linewidth on the alignment key and about 10 µm for a feature in the device region. These dimensions are approximate based on the photoresist and its sloped edges obtained after patterning, not based on the mask feature sizes.

In preparation for SEM inspection, chromium metal was flash evaporated on the photoresist for Wafers 1 and 2. Then the wafers were cleaved through the patterned photoresist features to obtain a piece from each wafer to be used as a sample to observe SEM cross sections of the photoresist. The imaging was done in the Zeiss Auriga SEM. Each sample was mounted onto a 45° sample holder.

Once loaded into the SEM vacuum chamber, the imaging was obtained using an electron-gun voltage of 2.5 kV (electrical high tension) to turn on the electron beam with an initial working distance of the sample from the cathode of about 1 cm. Detector SE2 was selected; the scan speed was set to 6; magnification was set to 20×; and brightness, contrast, magnification, focus, X, Y, Z, and theta were optimized. The cross section was put into position for imaging, and the beam was focused on a small particle/defect to optimize the image at high magnification using procedures similar to those used at 20×. Once the desired resolution of the particle/defect was obtained, the cross section was surveyed. Using a secondary electron (SE) SE2:in-lens ratio of about 2:8, a blend SE and in-lens camera imaging was obtained in order to see a balance of surface and depth in the image resolution.

SEM images of uncured and UV-cured photoresist were used to compare their overall film quality and study:

1) Top surface angle relative to wafer plane
2) Sidewall angle at bottom surface angles
3) Lateral distance between the top corner to top corner and the bottom corner to bottom corner.

A preliminary comparison of these profile properties to those obtained for the profilometer scans was performed.

3 Results/Discussion

3.1 Stylus Profilometry of Wide and Narrow Linewidths

Two types of photoresist linewidths were explored using a KLA Tencor P-15 profilometer with a 2-µm stylus. One rather large (~60 µm wide) and the other small (~10 µm). For the 60-µm feature size, the linewidth for the uncured resist is fairly well defined with little deviation from the desired cross-sectional profile, only slight rounding at the left and right transitions between the flat top and sloped edges (Figs. 1 and 2). The UV-cured case, however, shows a bumping up of the profilometer scan at the left and right transition between the flat top and sloped edges (Figs. 3 and 4). For the 10-µm feature size, the overall shape of the profilometer scan is more rounded at the sloped edges of the line, but the roundedness is more pronounced for the UV-cured versus uncured case (Figs 7 and 8 vs. Figs 5 and 6, respectively). Table 2 lists the critical dimensions for the scans. The scan of the uncured line has a 2-µm-wide plateau at the top, smaller than the desired 10 µm. The UV-cured case is fully rounded at the top with no such plateau. In both cases, the majority of the line is in the sloped region, and the impact of the stylus path over the photoresist needs to be factored in to realize this is not a faithful reproduction of the exact line shape. Nevertheless, it is a good first-order representation of the line shape.

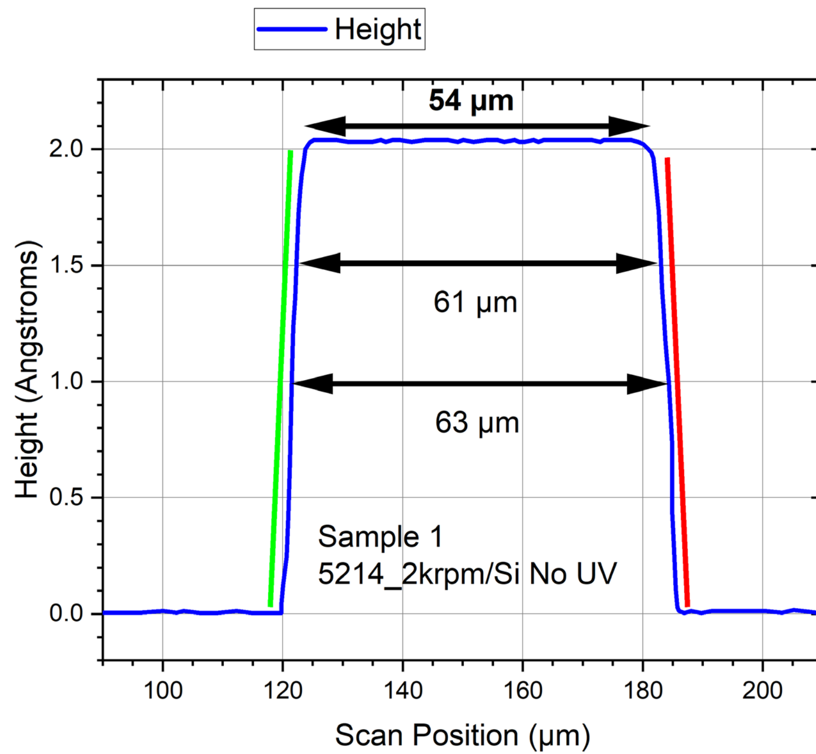

Fig. 1 Profilometer scan of the 60-µm (nominal) photoresist line for Wafer 1 (no UV cure)

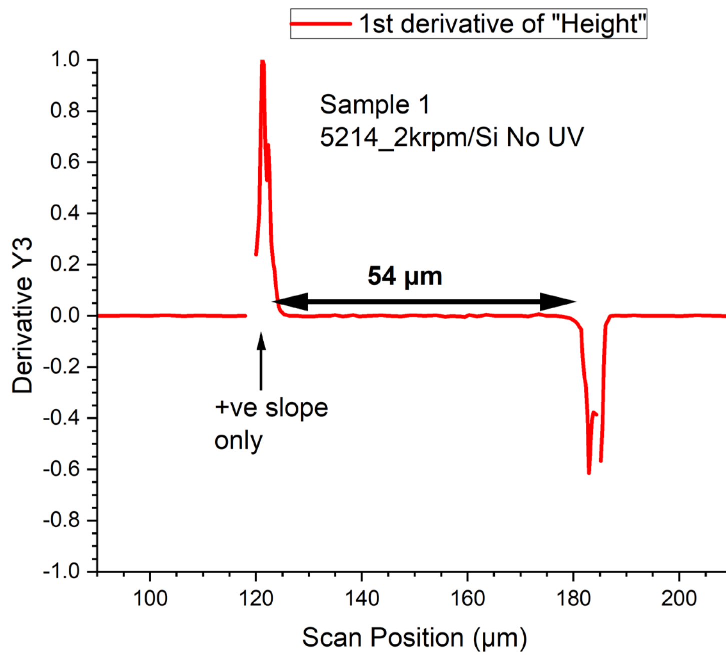

Fig. 2 Slope of the profilometer scan in Fig. 1. Gaps in the plot are an artifact in the local calculation of the derivative.

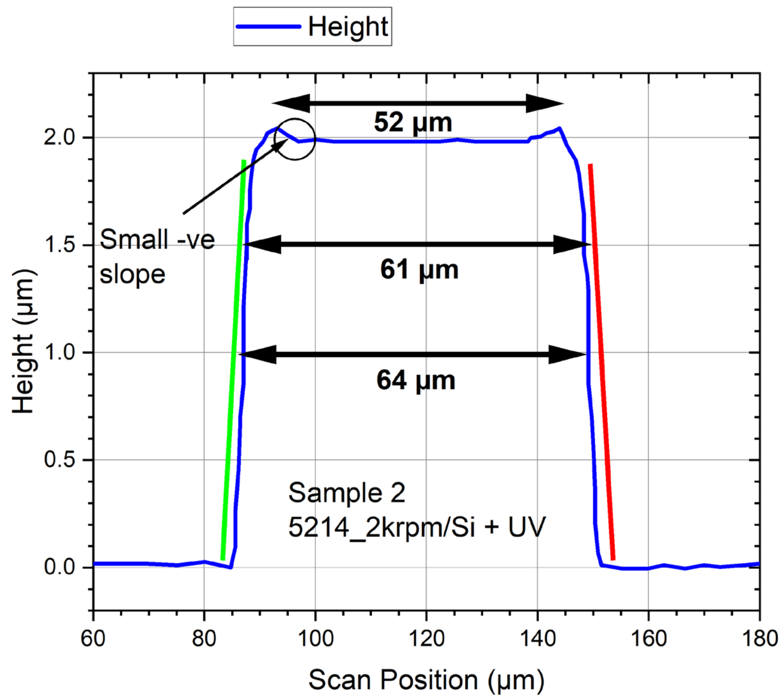

Fig. 3 Profilometer scan of the 60-µm (nominal) photoresist line for Wafer 2 (with UV cure). Measurement lengths corner-to-corner for Table 2 are illustrated as the red and green lines.

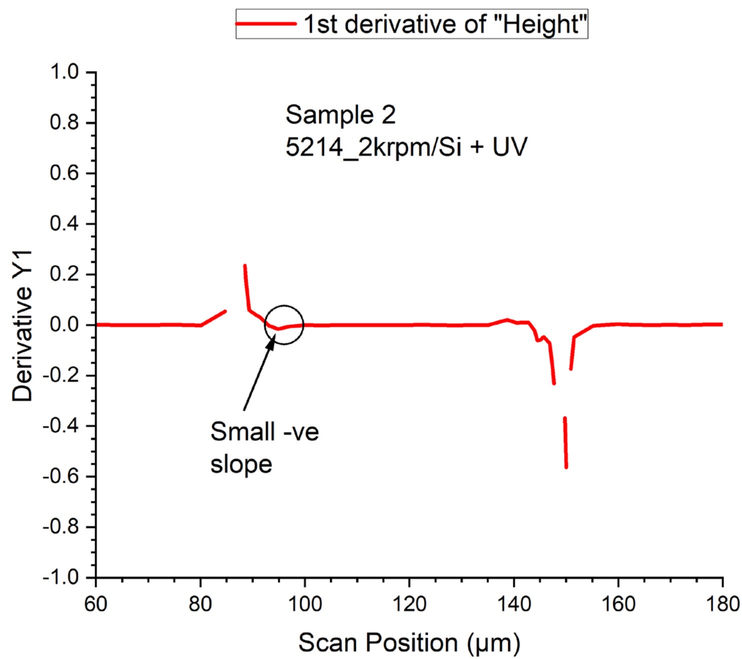

Fig. 4 Slope of the profilometer scan in Fig. 3. Gaps in the plot are an artifact in the local calculation of the derivative.

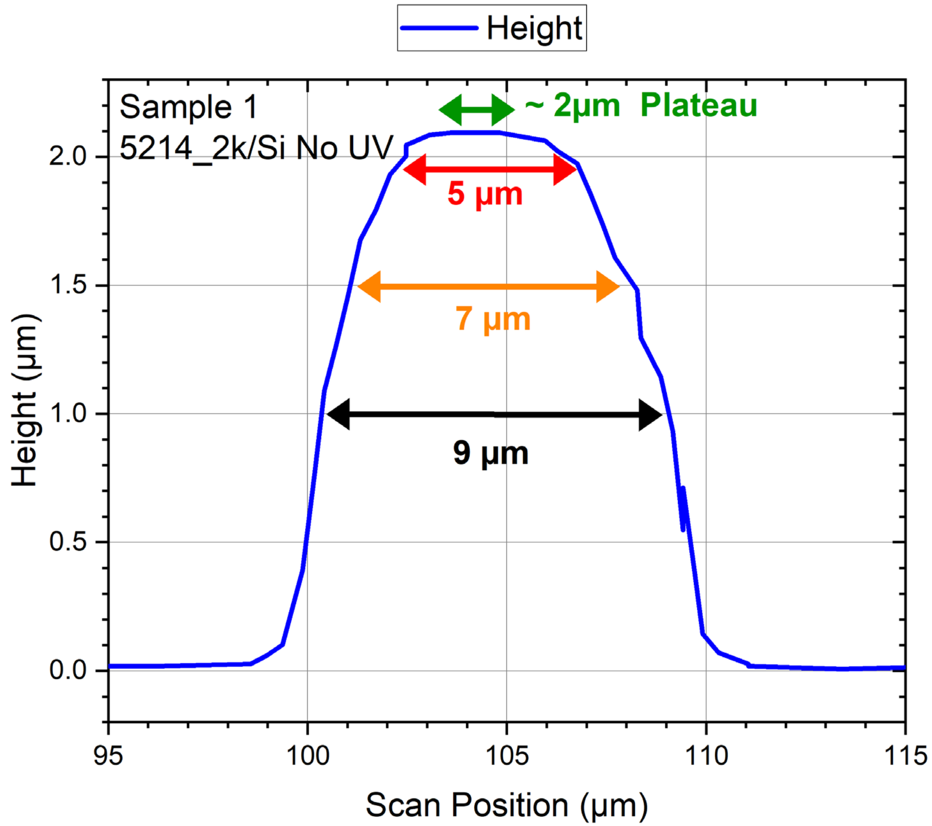

Fig. 5 Profilometer scan of the 10-µm (nominal) photoresist line for Wafer 1 (no UV cure)

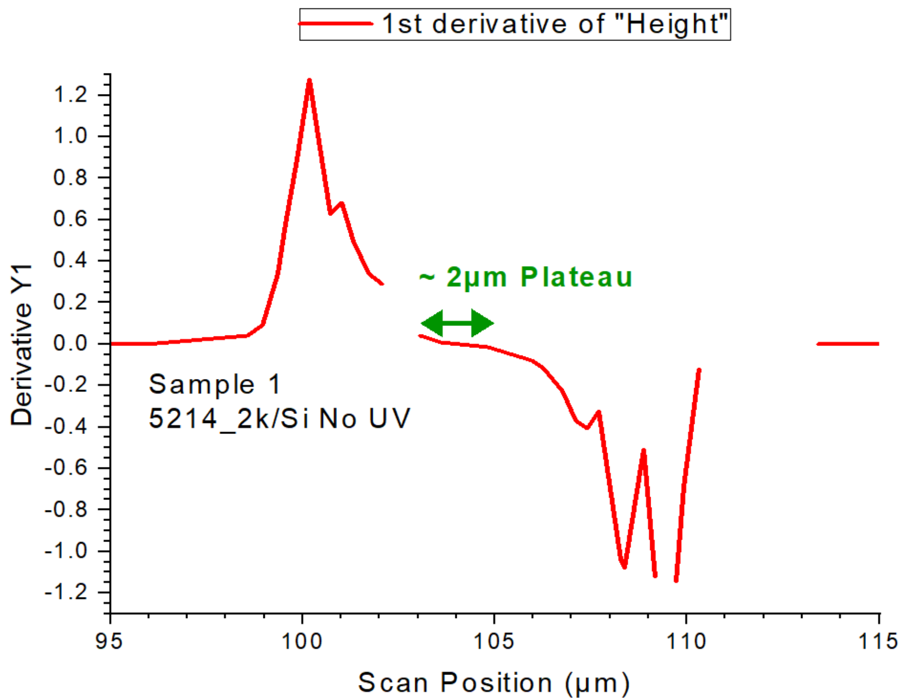

Fig. 6 Slope of the profilometer scan in Fig. 5. Gaps in the plot are an artifact in the local calculation of the derivative.

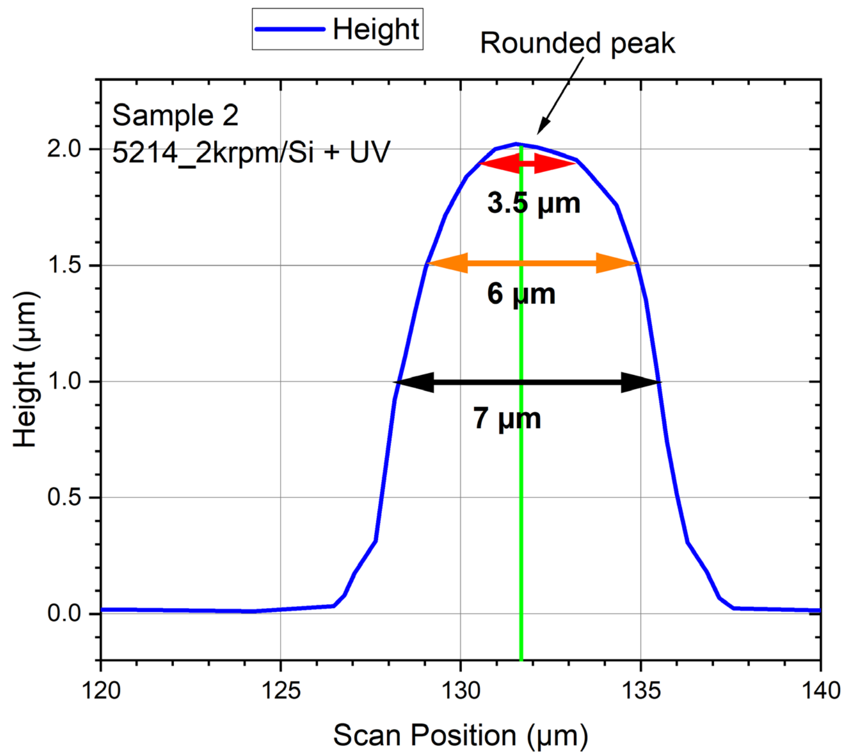

Fig. 7 Profilometer scan of the 10-µm (nominal) photoresist line for Wafer 2 (with UV cure)

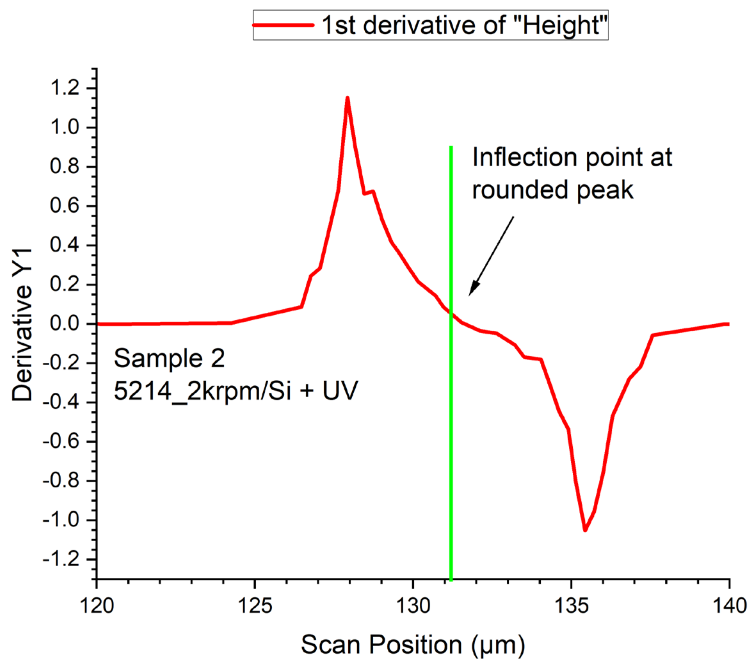

Fig. 8 Slope of the profilometer scan in Fig. 7

Table 2 Critical dimensions for the KLA Tencor P-15 profilometer scans obtained with a 2-µm stylus

ID	Vertical resist thickness (µm)	Top angle (deg)	Bottom angle (deg)	Top linewidth (µm)	Base linewidth (µm)	LHS top to bottom corners[a] (µm)	RHS top to bottom corners[b] (µm)
1_1 wide	2.036	19.498	19.498	55.25	67.63	5.75	6.50
1_2 narrow	2.080	20.716	20.716	2.50	14.00	5.25	5.75
2_1 wide	1.98 (C)	13.901	13.901	52	67	8	8
	2.029 (E)	…	…	…	…	…	…
2_2 narrow	2.014 (C)	19.345	19.345	4	12.5	5.75	5
	1.887 (E)	…	…	…	…	…	…

[a] See, for example, the length of the green line in Figs. 1 and 3.
[b] See, for example, the length of the red line in Figs. 1 and 3.
Note: C = through the vertical center of the linewidth, E = vertically through at the edge of the linewidth (though the center of the bump-up in the wide case), LHS = lefthand side, RHS = righthand side.

The image in Fig. 9 is from Hitachi and describes a stylus profile versus SEM cross-sectional image. It is instructive to consider the profile shape encountered for photoresist with sloped edge regions for both cases in order to best interpret how the profilometer scan deviates from the actual profile shape (which the SEM cross section more faithfully reproduces). This is important for informing the process and design rules.

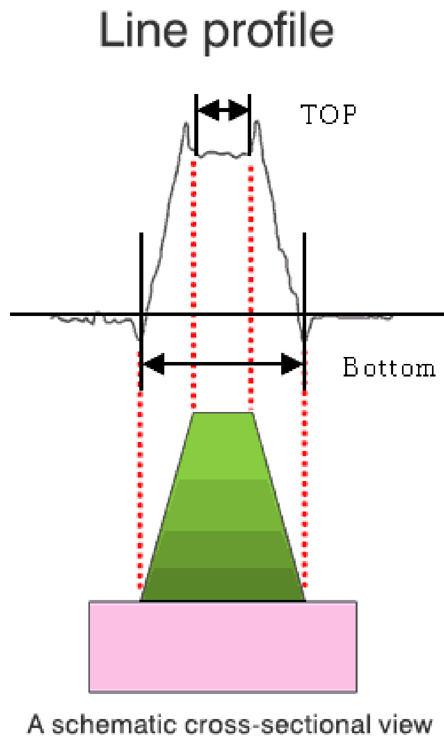

Fig. 9 Relationship between the line schematic cross-sectional view and the line profile[3]

3.2 SEM Images

The main difference in the broad area analysis between the uncured (not heat treated) and cured photoresist (heat treated in the Axcelis) is the smoothness of the sloped region for the uncured case compared to a pattern of ridges and furrows along the direction of the slope for the photoresist that was cured in the Axcelis (Figs. 10 and 11). Preliminary analysis of dimensions of the resist profiles for the SEM images were very different from those obtained using the profilometer. Since the SEM images were taken with the cross section off from the normal due to the rotation limits for the stage used, the perspective must be accounted for. A new set of SEM measurements obtained for the cross section normal to the beam would eliminate perspective issues so that dimensions in the SEM images can be directly and more accurately compared to those from the profilometer scans.

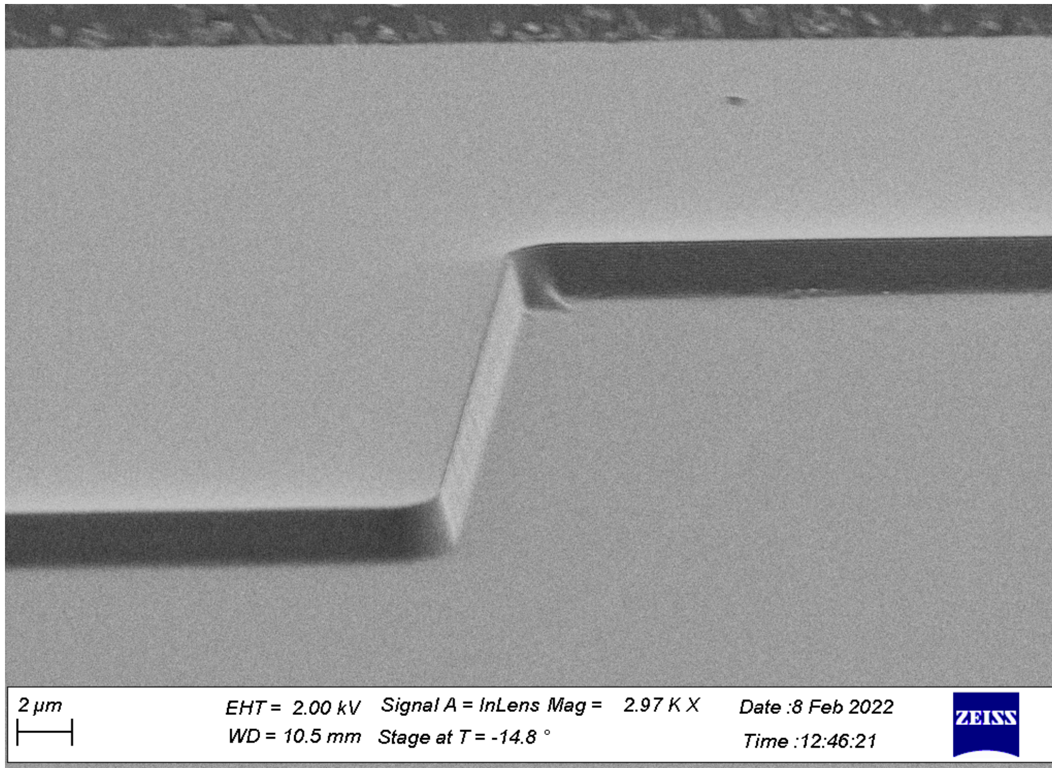

Fig. 10 Uncured photoresist (Wafer 1)

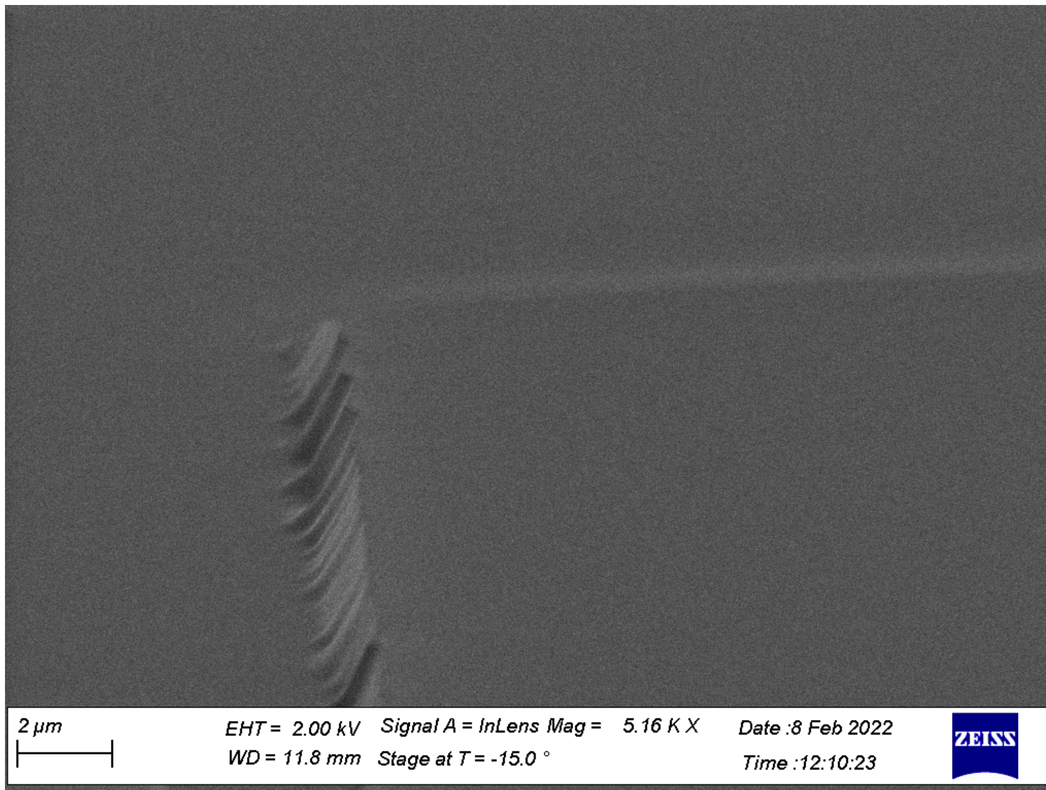

Fig. 11 UV cured photoresist (Wafer 2)

3.3 Options for Optimization Paths Forward

3.3.1 UV Cure Optimization of the Axcelis Process

3.3.1.1 Photoresist Stabilization Overview

Depending on the purpose of the resist mask, it may be appropriate to chemically or physically stabilize the developed resist structures by suitable means. This can be done either by means of a baking step for the thermal cross-linking of the entire resist structures, called hard bake, or via a combination of low-UV radiation and elevated temperatures, which cross-links the resist via both deep UV and hardening. This combination of UV radiation exposure and thermal heating is the procedure used for this report because of its effective track record in protecting against damage (in prior process work) from ion milling, deep reactive ion etch (DRIE), and other harsh processes used for thin-film removal. In both cases, thermal softening and rounding of the resist structures can occur, intended or undesired, called reflow.[4]

From an unpublished Axcelis tech report, options for optimizing UV cure of photoresist include the following:

- Best process results and throughput will be achieved using the D-Mod bulb. (DEVCOM Army Research Laboratory uses H-Mod), which has less UV energy below 300 nm compared to the H-Mod bulb and is thus able to more readily penetrate deeply into thick photoresists.
- Idle temperature is critical in controlling blisters and sidewall profiles. Start with the manufacturer's recommended soft-bake temperature for the resist.
- It is recommended the ramp rate should be at or near the tool's lower limit of 0.5 °C/s. Our ramp rate is higher (1–2 °C/s in the 110–200 °C range) (Table 3). Our initial and final ramp rates are ambiently controlled and not quantified.
- An oxygen purge will help eliminate reticulation and improve sidewall taper.
- Lamp high power can be increased to improve sidewall profiles (see first bullet).
- Use two-temperature plateaus. Our process currently uses three-temperature plateaus (Table 3).

Table 3 Ramp rates and temperature plateaus used

Rate (°C/s)	Temp change range (°C)
Rapid	21–110
2	110–150
1	150–170
1.5	170–200
Rapid	200–21

3.3.2 Hard Bake Alternatives

3.3.2.1 AZ Hard Bake for Cross-Linking

Hard bake makes the resist structures more stable during subsequent physical or chemical processes in the resist, such as wet or dry etching or electroplating. This raises the question of the optimum baking temperature for a given process.

Figure 12 shows solvent removal below 120 °C and thermal cross-linking above 130 °C. Upon exposure to light, diazonaphthoquinone (DNQ) converts to a derivative that is susceptible to etching. The data in Fig. 12 is specific to AZ 9260. However, it shows general properties and trends applicable to standard positive photoresists such as AZ 5214 studied here, though exact solubilities and threshold temperature for solvent reduction transition to cross-linking may differ.

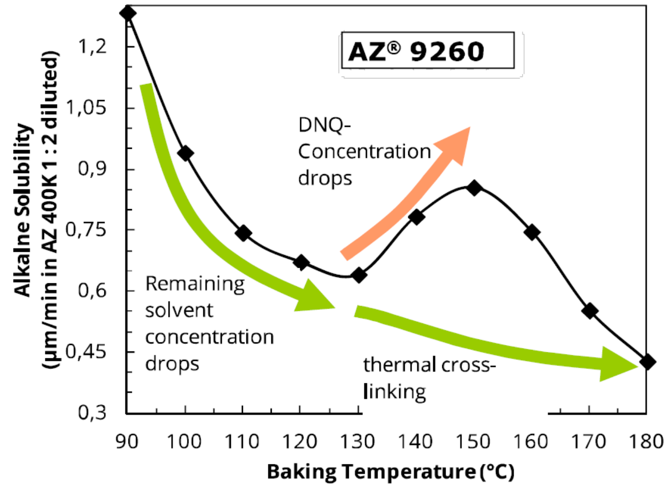

Fig. 12 A hard bake typically triggers various physical and chemical reactions in a resist film. At temperatures above 140 °C, positive resist film structures cross-link to increase their chemical stability for subsequent process steps.[5]

Figures 13 and 14 illustrate the possibility of deformation of the resist for hard bakes with temperatures in the range of 110–130 °C. While the resists shown in these figures are not AZ 5214 and are an order of magnitude thicker than the resist films deposited for this report, the potential for softening of the photoresist due to hard bake (above 110 °C for most standard photoresists) could be overcome and better hardening achieved by adding a UV-hardening component to the processing.

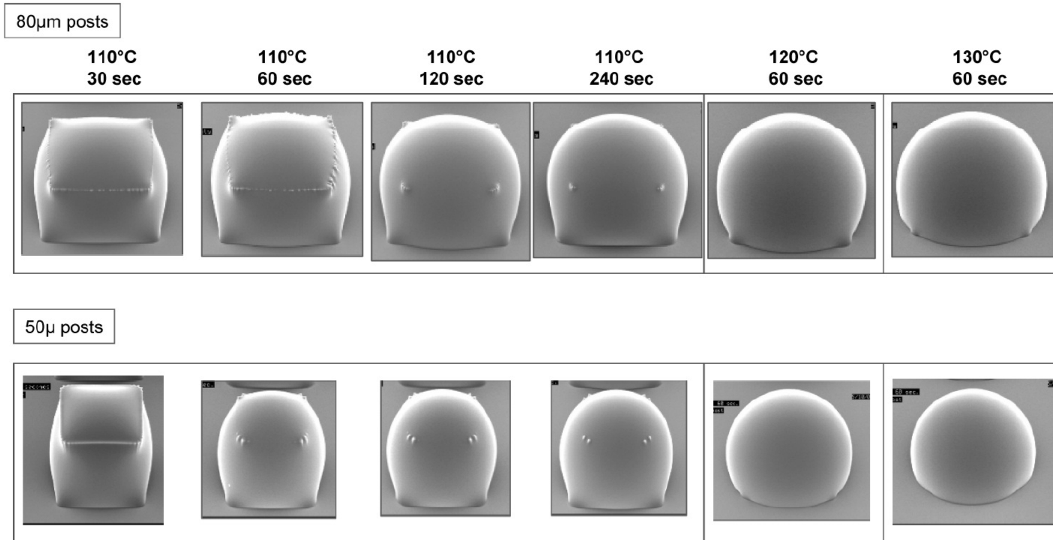

Fig. 13 The thermal softening (reflow) of developed rectangular resist structures from AZ 40XT at different temperatures and times for 80-µm resist film thickness (above) and 50-µm resist film thickness (below).[5]

Figure 14 shows better sidewalls for 110 °C or lower.

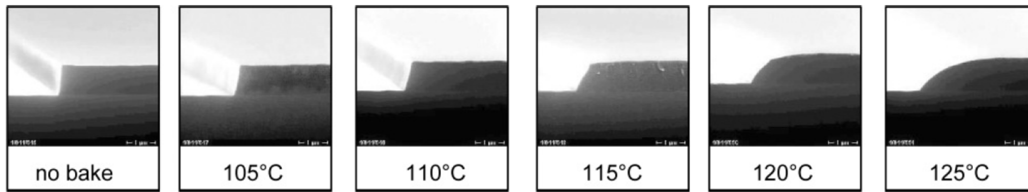

Fig. 14 Cross sections of thermally softened AZ ECI 3027 resist structures for increasing temperature, left to right[5]

3.3.2.2 Deep UV Hardening Not Achieved Using an Aligner Bulb Even for a Flood Exposure

Deep UV hardening using an aligner bulb (instead of the Axcelis process studied in this report) may be insufficient to achieve the desired photoresist toughness to withstand harsh processes such as DRIE and DSE. The following discussion notes the limitations and challenges.

3.3.2.3 Mechanism and Limits

Radiation around 250-nm wavelength breaks resin molecules of the photoresist, subsequent heating (stepwise or ramp-shaped on a hotplate, starting below the softening point followed by 10 °C steps upward) leads to cross-linking of the resist structures.

Due to the low penetration depth of the short-wave radiation, a few 10-nm-thick, cross-linked "crust" is formed on the resist surface, which protects the photoresist structure to a certain degree from thermal flow. If there is no special radiation source for deep UV radiation, a standard mask aligner can also be used for g-, h-, and i-line exposure. Here, however, the proportion of radiation around 250 nm is so small that a flood exposure (without mask) may be necessary for several hours in order to show a (possibly still small) impact. It should also be noted that the removability of the photoresist film through the cross-linked surface can be significantly worsened. AZ 5214E or AZ 9260 are not sensitive at g-line. See the spectral sensitivity chart in Fig. 15.

Spectral Sensitivity

The optical absorption (fig. right-hand) of unexposed positive photoresists ranges from approx. 460 nm in the VIS to near UV, which is matched to the emission spectrum of Hg lamps in mask aligners. This absorption spectrum causes the typical reddish-brownish colour of many photoresists. During exposure, photoresists almost completely bleach down to approx. 310 nm.Some modern positive resists such as the **AZ® 5214E** or **AZ® 9260** are not sensitive at g-line, while most negative resists such as the **AZ® nLOF 2000 series**, or the **AZ® 15nXT** and **125nXT** are only sensitive near i-line and therefore appear almost uncoloured to the human eye.The optical absorption range does not end abruptly towards higher wavelengths. Therefore, high illumination intensity (e. g. laser scribing) or -times allow an exposure also some 10 nm towards the visible part of the spectrum.Some resists such as the **PL 177** or **AZ® 520D** are dyed which makes it more easy to inspect the coating result.

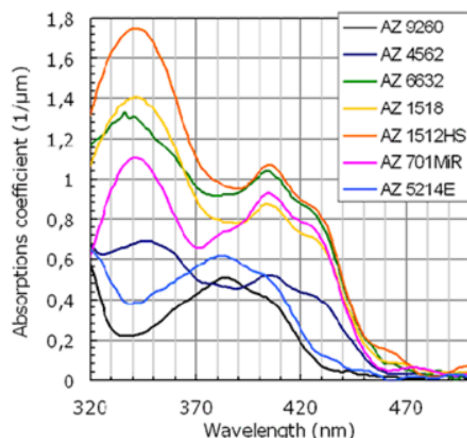

Fig. 15 Spectral sensitivity of AZ photoresists[6]

3.3.3 G-, H-, and I-Line Sensitive Photoresists

A number of photoresist types have specific frequency ranges of relative photoactivation (Table 4).[7]

Table 4 Frequency ranges of relative photoactivation

B line	Wave (nm)
g-	435
h-	405
i-	365

3.3.3.1 Broadband Resists

The spectral sensitivity of the AZ and TI photoresists is in the near-UV range (300–400 nm), and with most resists, also in the visible short-wavelength spectral range (blue: 450–495 nm).

3.3.3.2 I-Line Resists

Resists that are only sensitive in the range of the i-line (365 nm) are called i-line resists. These include, among others, chemically amplified positive resists such as AZ 40XT or negative resists such as AZ 15 nXT, AZ 125 nXT, or the AZ nLOF 2000 series. Broadband resists also absorb the g- (435 nm) and h- (405 nm) lines, but can also be exposed monochromatically within their spectral sensitivity.

3.3.3.3 Deep-UV Resists

Deep-UV resists have a spectral sensitivity below the 280-nm wavelength. Through exposure wavelengths of, for example, 247 or 193 nm, the resolution of attained resist structures can be improved significantly compared with i-line or broadband resists.

4. Summary and Conclusion

Optimization of UV cure is a desired approach in order to continue to reap the benefits of toughening the resist against attacks by the process it would be used in to protect the device features being patterned in materials such as PZT and aluminum nitride (AlN) piezoelectric materials. Further SEM analysis and tests on various substrate types are important considerations for the next steps in this study. Photoresist baking provides crosslinking that may require better optimization, but an absence of UV hardening may not provide the level of robust toughening that UV cure plus baking achieves. Also, photoaligner bulbs provide low UV output and so are not desirable alternatives to the Axcelis process.

Though it is beyond the scope of the study in this report, it is worth mentioning that alternative photoresists may have a role. However, to date, they are not tailored to the piezoMEMS processes used at DEVCOM ARL, and further testing is required to see if they are promising or unusable. Using optional resists, such as SPR,[8] for DSE etch has been considered by the team, as well as replacing AZ 5214 and AZ 9245 with SPR for the DSE etch. DEVCOM ARL also plans to evaluate AZ 4330.

5. References

1. UV photoresist curing systems Unihard. Ushio America, Inc; 2022 [accessed 2022 Aug 9]. https://www.ushio.com/product/uv-photoresist-curing-systems-unihard/.

2. Takacs TP, Pulskamp J, Polcawich R. UV baked/cured photoresist used as a sacrificial layer in MEMS fabrications. Army Research Laboratory (US); 2005 Feb. Report No.: ARL-MR-602.

3. CD-SEM - What is a critical dimension SEM? Hitachi; 2002 [accessed 2022 Aug 9]. https://www.hitachi-hightech.com/global/products/device/semiconductor/cd-sem.html.

4. MicroChemicals. Application notes. MicroChemicals; n.d. [accessed 2022 Aug 9]. www.microchemicals.com/downloads/application_notes.html.

5. Basic of microstructuring: hardbake, reflow and DUV hardening. MicroChemicals; n.d. [accessed 2022 Aug 9]. https://www.microchemicals.com/technical_information/photoresist_hardbake_reflow_uv_hardening.pdf.

6. Resists and developers. MicroChemicals; 2013 Nov 17 [accessed 2022 Aug 9]. https://www.microchemicals.eu/technical_information/resists_developers.pdf.

7. Basic of microstructuring: exposure. MicroChemicals; n.d. [accessed 2022 Aug 9]. https://microchemicals.com/technical_information/exposure_photoresist.pdf.

8. MEGAPOSIT SPR 220 series photoresists for i-line applications. Rohm and Haas; 2004 [accessed 2022 Aug 9]. https://research.engineering.ucdavis.edu/cnm2/wp-content/uploads/sites/11/2013/05/SPR220_Data_Sheet.pdf.

List of Symbols, Abbreviations, and Acronyms

AlN	aluminum nitride
ARL	Army Research Laboratory
AZ	Azoplate; brand of photoresist
DEVCOM	US Army Combat Capabilities Development Command
DNQ	diazonaphthoquinone
DOE	design of experiment
DRIE	deep reactive ion etch
DSE	deep silicon etch
g-line	435-nm wavelength
h-line	405-nm wavelength
HMDS	hexamethyldisilazane; a surfactant applied to a surface to enhance adhesion prior to coating it with photoresist.
i-line	365-nm wavelength
in lens detector	immersion lens detector for SEM imaging; in-lens SEM detectors mostly collect the secondary electrons induced by the primary electron beam (SE1 secondary electrons).
LHS	lefthand side
MEMS	microelectromechanical systems
Piezo	piezoelectric
PZT	lead zirconate titanate
resist	photoresist
RHS	righthand side
SE	secondary electron
SE2 detector	secondary electron detector for SEM imaging which collects backscattered (SE2) secondary electrons.
SEM	scanning electron microscopy
Si	silicon

SiO_2	silicon dioxide
SPR	brand of photoresist
UV	ultraviolet

1 DEFENSE TECHNICAL
(PDF) INFORMATION CTR
DTIC OCA

1 DEVCOM ARL
(PDF) FCDD RLD DCI
TECH LIB

11 DEVCOM ARL
(PDF) FCDD RLS SA
D POTREPKA
P SUNAL
J PULSKAMP
R BENOIT
R RUDY
R KNIGHT
G SULLIVAN
B POWER
I KIERZEWSKI
FCDD RLS T
R BURKE
FCDD RLS F
A COHEN